

BNL--39661

DE87 010071

2

REVIEW OF THE BROOKHAVEN NEUTRINO WORKSHOP

Michael J. Murtagh
Department of Physics, Brookhaven National Laboratory
Upton, New York 11973
USA

Invited talk given at
Lake Louise Winter Institute's Topical Conference
Lake Louise, Canada, Feb. 19-21, 1987

DISCLAIMER

This report was prepared as an account of work sponsored by an agency of the United States Government. Neither the United States Government nor any agency thereof, nor any of their employees, makes any warranty, express or implied, or assumes any legal liability or responsibility for the accuracy, completeness, or usefulness of any information, apparatus, product, or process disclosed, or represents that its use would not infringe privately owned rights. Reference herein to any specific commercial product, process, or service by trade name, trademark, manufacturer, or otherwise does not necessarily constitute or imply its endorsement, recommendation, or favoring by the United States Government or any agency thereof. The views and opinions of authors expressed herein do not necessarily state or reflect those of the United States Government or any agency thereof.

MASTER

DISTRIBUTION OF THIS DOCUMENT IS UNLIMITED



REVIEW OF THE BROOKHAVEN NEUTRINO WORKSHOP

Michael J. Murtagh
Department of Physics, Brookhaven National Laboratory
Upton, New York 11973
USA

ABSTRACT

Recent experimental results on searches at accelerators for $\nu_{\mu} \rightarrow \nu_e$ oscillations presented at the Brookhaven National Laboratory Neutrino Workshop are reviewed and prospects for extending these searches are discussed.

1. INTRODUCTION

The primary objectives of the Neutrino Workshop held at Brookhaven National Laboratory¹⁾ were to review recent progress in neutrino physics as it relates to the present BNL AGS program and to investigate possible future neutrino experiments at BNL which could profitably use the enhanced flux available when the Booster project²⁾ is completed. The present AGS wide band neutrino beam is a fast spill (2.4 μ sec) beam with a 1.4 sec rep rate and approximately $1.5 * 10^{13}$ protons per pulse delivered to the neutrino target. When the new Booster ring is completed (\approx 1990) it is expected that the number of protons per pulse available will increase by at least a factor of four.

This report will be limited to a review of recent experimental results on searches at accelerators for $\nu_{\mu} \rightarrow \nu_e$ oscillations and to a discussion of future prospects for expanding these searches. While this was the central topic in the workshop, many other aspects of neutrino physics were discussed. Recent theoretical work on the

theory of neutrino oscillations with 3-flavor mixing and the implications for accelerator experiments in light of the recent matter oscillation solutions for the solar neutrino problem were discussed. Variations in neutrino oscillations caused by the passage of the neutrinos through the earth were also reviewed. An extensive comparison of the standard model of electroweak interactions with present experimental data was presented. The agreement between the theory and over a hundred experimental results is excellent and one can use this agreement to place rather stringent constraints on the allowed masses of many hypothetical particles (e.g. top, Higgs, Z' etc.). In many ways the success of present theory makes it difficult to envision significant new non-oscillation neutrino experiments in the BNL energy range. Prospects for low energy neutrino experiments were reviewed in the context of recent results on $\bar{\nu}_\mu e$ and $\bar{\nu}_\mu p$ elastic scattering from BNL experiment E734³⁾. There was also a report from the HRS collaboration at PEP⁴⁾ on evidence for the anomalous τ decay $\tau^+ \rightarrow \pi^+ \eta \bar{\nu}_\tau$ and the possibility that this is evidence for second class currents. Most of the discussion at the workshop on future experiments focussed on oscillation experiments. In addition to Long Baseline Experiments which are discussed below, there were working groups on Tagged Neutrino Beams and Appearance Searches for $\nu_\mu \rightarrow \nu_\tau$ Oscillation. The tagged neutrino beam would be a $K_L \rightarrow \lambda \pi \nu_e$ based beam in which the K_L is reconstructed on an event by event basis and in this way the species of neutrino identified. Present theoretical prejudice favors $\nu_\mu \rightarrow \nu_\tau$ as the oscillation most likely to be accessible in accelerator oscillation experiments. Since the BNL neutrino beam peaks at ≈ 1 GeV (10% of the beam is above 4 GeV), $\nu_\mu \rightarrow \nu_\tau$ appearance experiments appear very difficult. However, the extra flux provided by the Booster coupled with some distinctive signature for τ -decay may yield a feasible experiment. An alternative approach would be to do a disappearance experiment coupled with a measurement of neutral to charged current ratios.

2. $\nu_\mu \rightarrow \nu_e$ OSCILLATIONS

The probability that an electron neutrino (ν_e) with energy E_ν will be observed at a distance L from the source of a muon neutrino (ν_μ) beam is given by

$$P(\nu_\mu \rightarrow \nu_e : L; E_\nu) = \sin^2 2\alpha \sin^2(1.27 \Delta m^2 L/E_\nu)$$

where L is in meters, E_ν in MeV and Δm^2 in $(\text{eV})^2$. Experimentally $P(\nu_\mu \rightarrow \nu_e : L; E_\nu)$ is defined as the ratio of the excess number of electron events (n_e) to the number of muon events (n_μ). The excess electron events are the observed number of electron events corrected for the expected number of electron events in the original beam and the background due to photon conversions from π^0 decay simulating electron events. In the limit of very short wavelength (large Δm^2) one observes in the detector the average of many oscillations and the oscillation formula reduces to

$$\sin^2 2\alpha = 2 \times n_e/n_\mu.$$

In the limit of long wavelength (small Δm^2) the oscillation formula reduces to

$$\Delta m^2 \sin 2\alpha = 0.8 \times (E_\nu/L) \times \sqrt{n_e/n_\mu}.$$

In practice, most $\nu_\mu \rightarrow \nu_e$ appearance oscillation searches at accelerators have used a single detector. This is possible in large part because the expected ν_e contamination in the beam is small ($\approx 1\%$) and the ratio ν_e/ν_μ is calculable with reasonable precision ($\leq 20\%$). The ratio is essentially determined by the K/π ratio in the production spectra and is largely insensitive to uncertainties in other details of the beam operation. The dominant sources of ν_μ are $\pi \rightarrow \mu\nu$ and $K \rightarrow \mu\nu$ decays while the sources of ν_e are $\pi \rightarrow \mu \rightarrow e\nu_e\nu_\mu$, and $K^+ \rightarrow \pi e\nu_e$, $K_L^0 \rightarrow \pi e\nu_e$ decays. The relevant contributions to the ν_e spectrum at the location of the E734 detector for the wide-band neutrino beam at BNL are shown in Fig. 1. In this beam the dominant contribution is from the $\pi \rightarrow \mu \rightarrow e\nu\nu$ decay which produces a peak in the spectrum at a similar energy to the peak in the ν_μ spectrum.

While all experiments rely on calculations to determine the

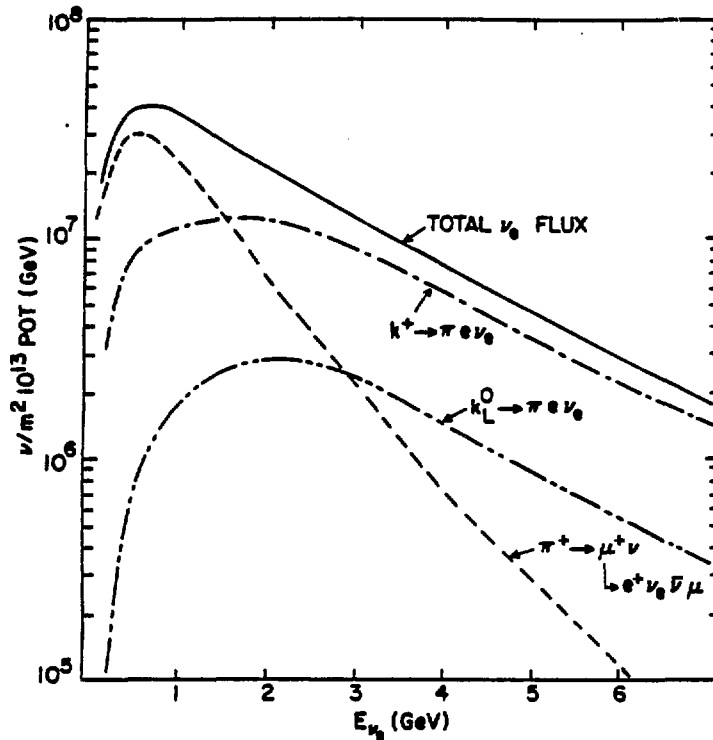


Fig. 1. Calculated ν_e spectrum for BNL wide band beam at the E734 detector.

expected ν_e flux in the initial beam, they have to measure the fake "e" contribution from photon conversion. The major sources of π^0 are charged (neutral) current single pion production which amounts to ≈ 0.4 (≈ 0.04) of the quasi-elastic cross-section in this energy range. By rejection complicated topologies and identifying π^0 at some level the experiments are able to reduce this background to less than the expected level of electrons from ν_e in the beam ($\approx 1\%$).

To establish the existence of $\nu_\mu \rightarrow \nu_e$ oscillations, it is necessary to observe a significant excess of electron events. In addition, the excess electron events must have the correct L/E_ν behavior. In a single detector experiment this would require measuring n_e/n_μ as a function of neutrino energy. Given the

uncertainties involved in measuring the expected n_e/n_μ background ratio, final confirmation would probably require observing the correct L/E_ν behavior in two similar detectors at two significantly different distances.

3. SUMMARY OF RESULTS

At the workshop two experimental groups^{5,6)} gave preliminary results on $\nu_\mu \rightarrow \nu_e$ oscillations in which they claim to observe a significant excess of electrons. The ranges in Δm^2 , $\sin^2 2\alpha$ space allowed by these preliminary positive results are shown in Fig. 2. Since neither group has completed their analysis and at the present time are not quoting systematic errors, these curves should be viewed as indications of the likely allowed regions when the final analysis is completed. Both groups believe that the significance of their observation will remain $\geq 3\sigma$.

Two other experiments^{7,8)} have recently published limits on $\nu_\mu \rightarrow \nu_e$ oscillations (Fig. 2) which appear to be in conflict with the claimed positive results.

A brief review of all four of these experiments follows.

4. THE BEBC $\nu_\mu \rightarrow \nu_e$ OSCILLATION SEARCH

An Athens, Padova, Pisa, Wisconsin collaboration⁸⁾ used the BEBC bubble chamber filled with a heavy neon/hydrogen mixture ($\rho \approx 0.7$ gm cm⁻³, $X_0 = 43$ cm) to search for $\nu_\mu \rightarrow \nu_e$ oscillations in a specially built single horn focussed neutrino beam from the CERN PS. This beam, produced by 19 GeV/c protons from the PS, had a mean energy of ≈ 1.5 GeV at the bubble chamber which was located ≈ 900 meters from the production target. The calculated ν_e/ν_μ ratio for this beam is $\approx 4 \times 10^{-3}$. The heavy liquid provides excellent electron identification (95% of e^\pm have > 2 signatures) and the high spatial resolution combined with the magnetic field essentially eliminates e/γ ambiguities.

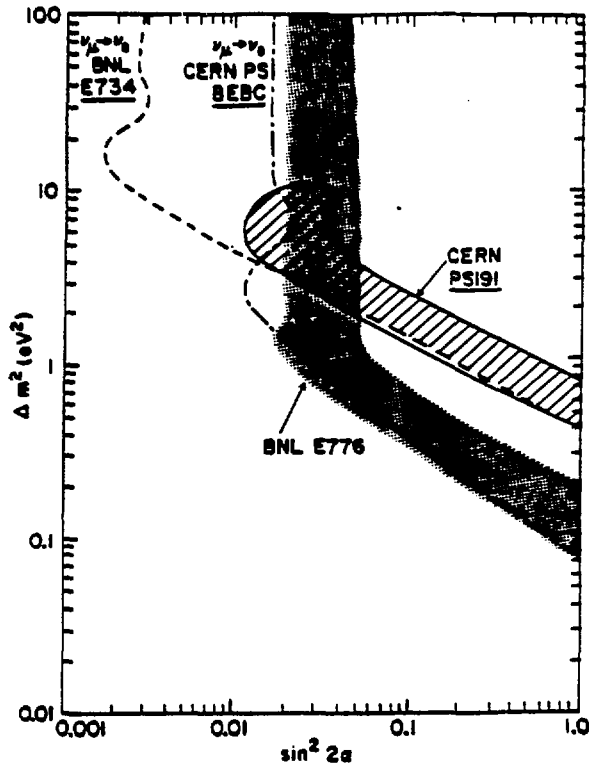


Fig. 2. Experimental results on $\nu_{\mu} \rightarrow \nu_e$ oscillations. Limits from BNL 734 (Ref. 7) and CERN BEBC (Ref. 8). Positive results from CERN PS191 (Ref. 9) which is in agreement with BNL E816 (Ref. 5) results and BNL E776 (Ref. 6). The E776 region is indicative of the allowed region but does not represent a confidence level contour.

Since the bubble chamber is live for a long time per spill and is far from the source, the neutrino event rate is low and the cosmic ray rate is high. In a total of 794,000 pictures, corresponding to $.9 \times 10^{19}$ protons on target, a total of 4017 event candidates were found. From a rescan of 60% of the film the overall scanning efficiency was determined to be 90%. The distribution of $\cos\theta$, where θ is the angle between \vec{P}_{VIS} (the vector sum of the measured track momenta) and the nominal beam direction for events with leaving negative (or stopping μ^-) tracks and a vertex in the fiducial volume, is shown in Fig. 3. A clear peak of beam induced events is observed at $\cos\theta = 1$ together with a broad distribution of cosmic ray events. Requiring that $|\vec{P}_{VIS}| > 200$ MeV/c, that there is a reasonable kinematic constraint ($E_{VIS} - P_{VIS} < 1$ GeV) in the beam direction and that $\cos\lambda > 0.8$, where λ is the dip angle, essentially removes the cosmic background as shown by the shaded region in Fig. 3. A final cut of $\cos\theta > 0.8$ produced a sample of 470 ν_{μ} charged current events

with an estimated background of 24 ± 5 events. The visible energy distribution of these events (Fig. 4) is in good agreement with the expected distribution from a Monte Carlo beam calculation. A total of 4 events in the final sample have identified final state electrons and are classified as ν_e events. The neutrino (electron) energies for these events are 2.5(1.5), 5.9(3.4), 2.8(2.0), 1.4(0.9) GeV. The expected number of ν_e induced events from the beam calculation is 3 so there is no significant excess of electron events to ascribe to oscillations. Furthermore, the energy distribution of the electron events is consistent with being beam induced background and does not have the L/E_ν behavior expected for oscillations. The resulting $\nu_\mu \rightarrow \nu_e$ oscillation limits from this experiment are shown in Fig. 2. For maximal mixing the limit is $\Delta m^2 < 0.09 \text{ eV}^2$ and for $\delta m^2 = 2.2 \text{ eV}^2$, the limit is $\sin^2 2\alpha < 0.013$ at the 90% confidence level.

5. THE E734 $\nu_\mu \rightarrow \nu_e$ OSCILLATION SEARCH

The E734 detector at Brookhaven was constructed by a USA-Japan collaboration comprised of physicists from BNL, Brown Univ., KEK, Osaka Univ., Univ. of Pennsylvania and SUNY at Stony Brook. The original proposal for this experiment was to measure the elastic scattering of neutrinos on electrons and protons. Since the emphasis in the design was on electron identification and e/γ separation, it is an excellent detector for a $\nu_\mu \rightarrow \nu_e$ oscillation search.

The E734 detector (Fig. 5) is a 175 ton target-calorimeter containing 112 modules followed by a lead-liquid scintillator shower absorber and a magnetic spectrometer. Each module contains a $4\text{m} \times 4\text{m} \times 7.5\text{cm}$ plane of liquid scintillator segmented into 16 horizontal cells followed by $4\text{m} \times 4\text{m} \times 3.75\text{cm}$ X and Y measuring planes of proportional drift tubes (each plane contains 54 PDT's). The liquid scintillator cells have phototubes on each end and multiple times and a single pulse height can be recorded for each spill. Two times and a single pulse height can be recorded for each PDT tube. Each module is $\approx 1/4$ radiation length and the detector is approximately 90% active. The high segmentation coupled with the timing and pulse height

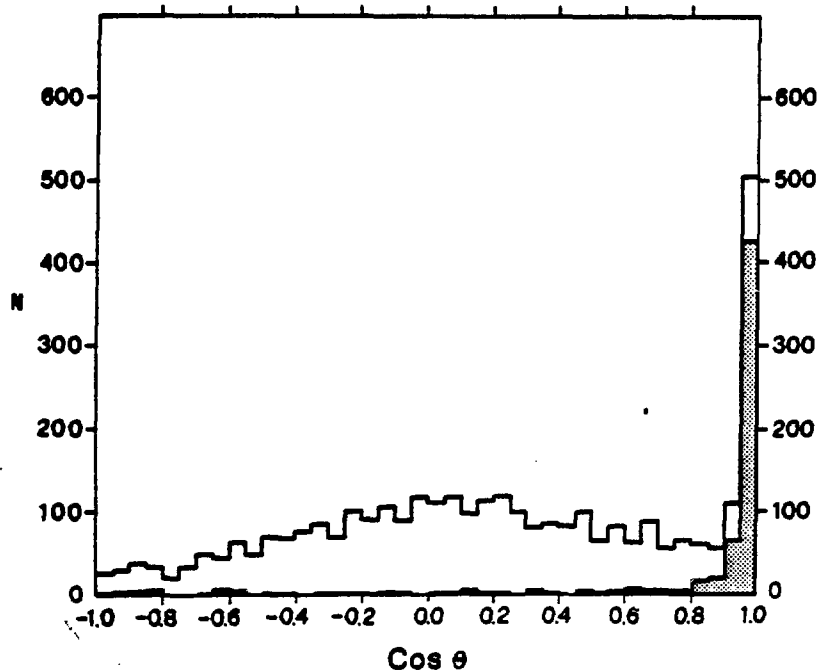


Fig. 3. Distribution in $\cos\theta$, the angle between the visible momentum vector and the beam direction for charged current event candidates. The shaded region shows the events remaining after cuts to remove cosmic rays.

information provides excellent π/p separation, electron identification and photon rejection. The detector is located at the end of the neutrino beam line with a mean distance from the center of the decay tunnel to the center of detector of 96 meters. Since the wide-band beam peaks at 1 GeV, the L/E_ν is 0.1.

In this experiment the ratio of ν_e quasi-elastics ($\nu_e n \rightarrow e^- p$) to ν_μ quasi-elastics ($\nu_\mu n \rightarrow \mu^- p$) is measured as a function on neutrino energy and compared to the calculated ratio. These events, in the low Q^2 region, appear in the detector as single tracks or showers with at most some low energy associated activity at the vertex and are very similar to neutrino elastic scattering events. The data beam bursts. Electron candidates were obtained by processing all bursts through a coarse computer filter program to retain events with any electromagnetic shower within 240 mrad of the neutrino beam direction. After scanning by physicists to remove events with additional hadron tracks or significant disconnected energy, a total

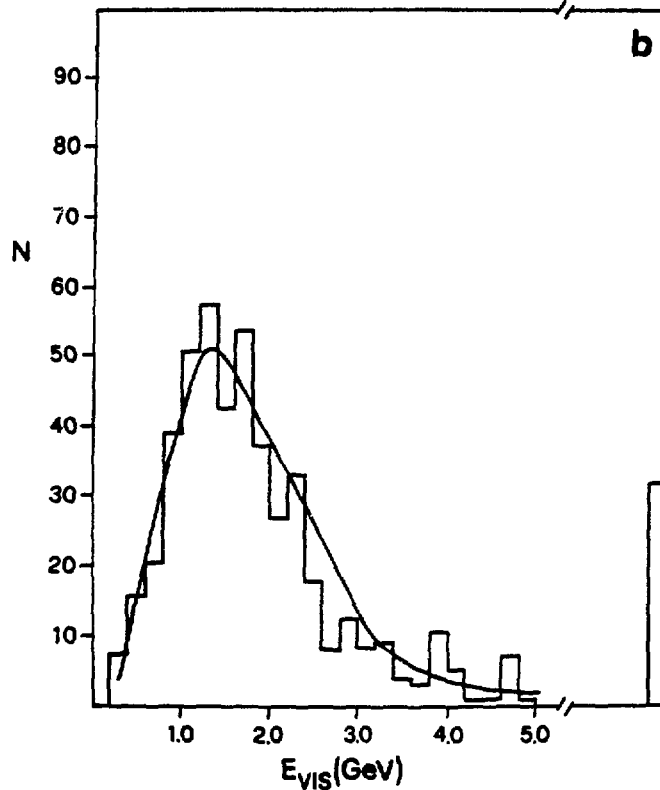


Fig. 4. Visible energy distribution of selected ν_{μ} charged current events. The curve is the expected distribution from a Monte Carlo calculation.

of 873 events with $\theta < 240$ mrad and $0.21 < E_e < 5.1$ GeV remained. The shower energies have a 40% correction for invisible energy and the energy resolution is $\Delta E/E = 0.12/\sqrt{E}(\text{GeV})$. The shower angle was determined from a fit to all shower hits in the PDT cells and the angular resolution was $\Delta\theta = 30$ mrad.

The major backgrounds in this sample are from $\nu N\pi$ neutral currents, inelastic ν_e scatters ($\nu_e N\pi$) and to a lesser extent $\nu_{\mu e} \rightarrow \nu_{\mu e}$ elastic scattering. Reactions with a π^+ in the final state were measured by observing the delayed signal from $\pi^+ \rightarrow \mu^+ e$ decay. The shower energy distribution for the events retained after the π^+ background events were subtracted is shown in Fig. 6a. During the scanning, events with a single shower associated with an upstream energy deposition were collected and used as a control sample of

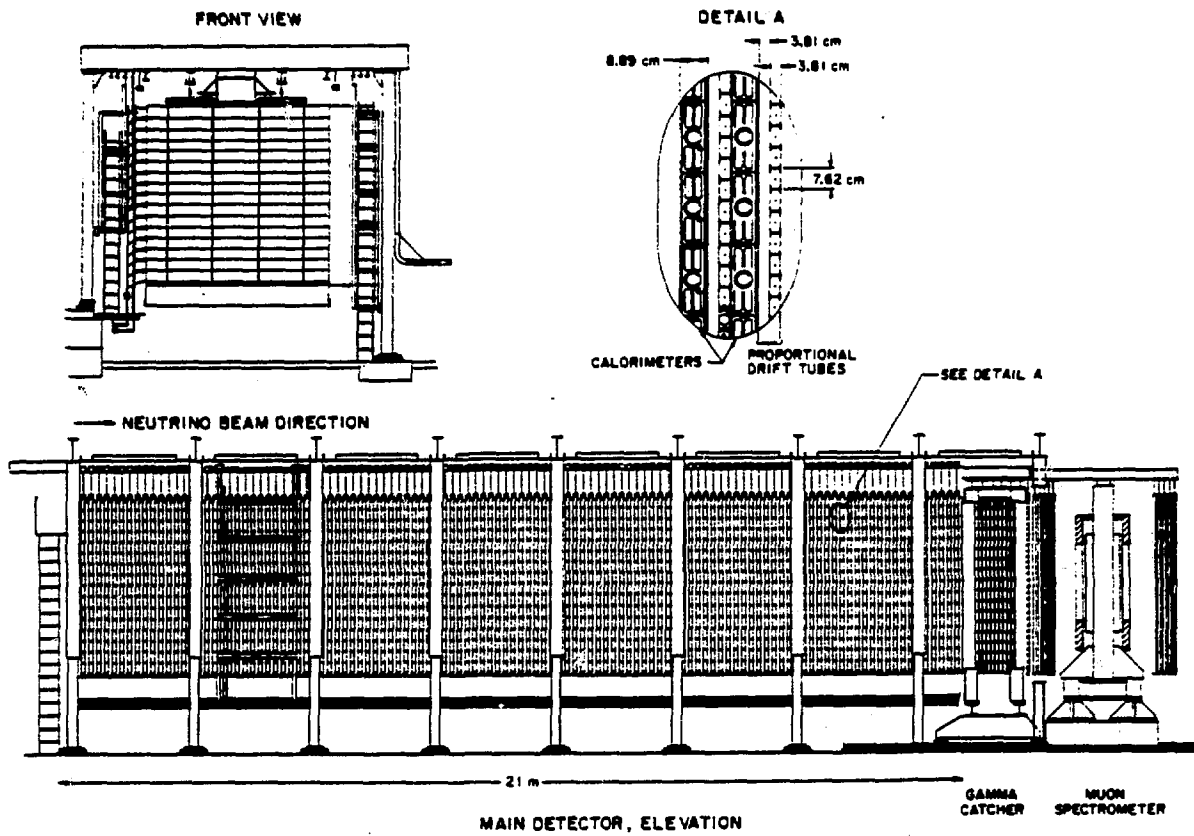


Fig. 5. The E734 detector.

identified photons. The shower energy distribution of these photons is given on Fig. 6b. The e^-p candidates (Fig. 6a) below 0.9 GeV are expected, from calculation and observation, to be mostly photons with a small number of $\nu_{\mu}e \rightarrow \nu_{\mu}e$ and very few low energy $\nu_e\mu \rightarrow e^-p$ because of the 240 mrad restriction. Therefore it is possible to subtract the photon induced events above 0.9 GeV in Fig. 6a by normalizing the distributions in Fig. 6a, 6b below 0.9 GeV. After subtracting events with observed π^+ decays and correcting for the π^+ decay efficiency (40% of candidates), removing π^0 's using the observed π^0 events (13%) and making small corrections for $eN\pi$ (3%) and $\nu_{\mu}e \rightarrow \nu_{\mu}e$ (5.8%), a total of 418 e^-p events remained.

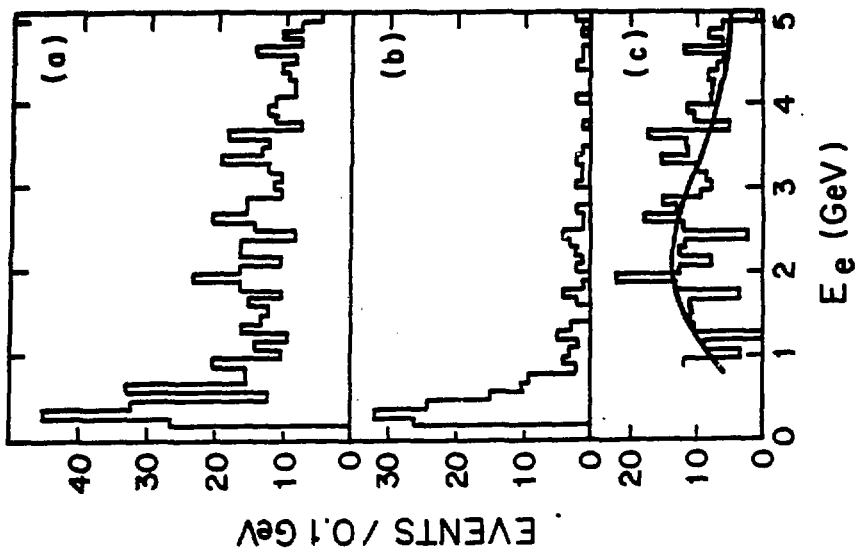


Fig. 6a. Shower energy distribution for all possible $\nu_e n + e^- p$ candidates; b. Shower energy of photons associated with upstream event vertex; c. The electron energy distribution after all background subtraction.

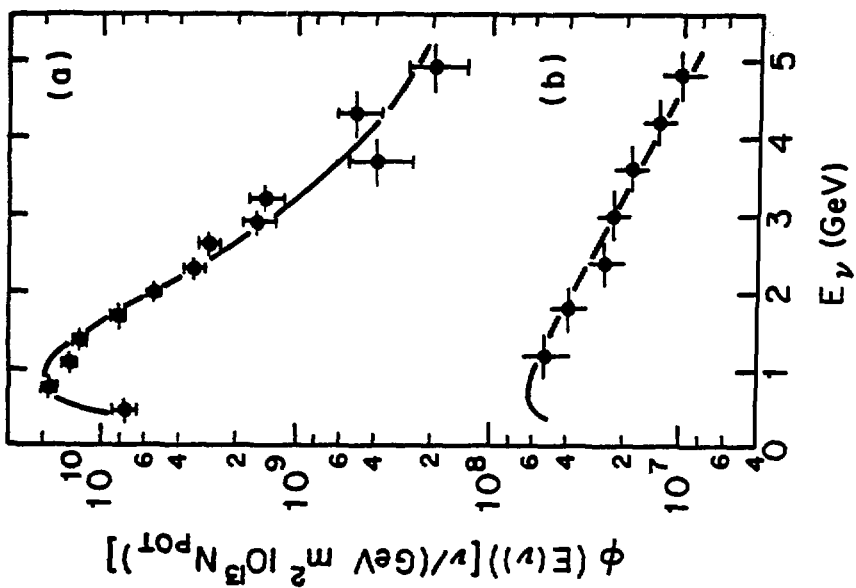


Fig. 7a. ν_μ flux obtained from $\nu_\mu n + \mu^- p$ events;
 b. ν_e flux obtained from $\nu_e n + e^- p$ events. The solid lines are the fluxes calculated from a neutrino beam program.

The ν_e events were normalized to a sample ($\approx 10\%$ of data) of 1370 $\nu_\mu n \rightarrow \mu^- p$ quasi-elastic events in which one long track left the detector and the other stopped in the detector and was identified by range and ionization as a proton. The background in this sample after acceptance criteria were applied, consisted of charged current single π^+ production (13% of $\mu^- p$ rate) and a small contribution ($\approx 3\%$) from π^0 and multipion production.

The neutrino spectra derived from these measured quasi-elastic samples are shown in Fig. 7 together with the calculated spectra. The agreement between the observed and calculated ν_μ spectrum in Fig. 7 is a check on the validity of the beam program and of the parameters for π and K production used in it. The agreement between the observed and calculated ν_e spectrum as a function of energy sets limits on possible $\nu_\mu \rightarrow \nu_e$ oscillations. To determine the oscillation limits only the ratio of fluxes is required. This ratio is shown in Fig. 8a and the difference between the measured and calculated ratios as a function of neutrino energy is shown in Fig. 8b. Clearly there is no evidence for oscillations. The errors on the data points include a systematic uncertainty of 20% (comprised of equal contributions from the flux calculation and the acceptance calculations). Using the data in the energy range $900 \leq E_\nu(\text{MeV}) \leq 2100$, the region in $\Delta m^2 - \sin^2 2\alpha$ space excluded with 90% confidence is shown in Fig. 2. The large Δm^2 limit is $\sin^2 2\alpha < 3.4 \times 10^{-3}$ while in the small Δm^2 limit $\Delta m^2 \sin 2\alpha < 0.43 \text{ eV}^2$ at the 90% confidence level.

6. THE E816 $\nu_\mu \rightarrow \nu_e$ OSCILLATION EXPERIMENT

Experiment E816, a Boston Univ., BNL, CERN, Paris collaboration, to search for $\nu_\mu \rightarrow \nu_e$ oscillations in the wide band beam at Brookhaven with a detector located at $\approx 100\text{m}$ is a continuation of a similar search using the PS beam at CERN. In the CERN experiment (CERN PS191, an Athens, CERN, Paris, Rome collaboration⁹) an excess of ν_e

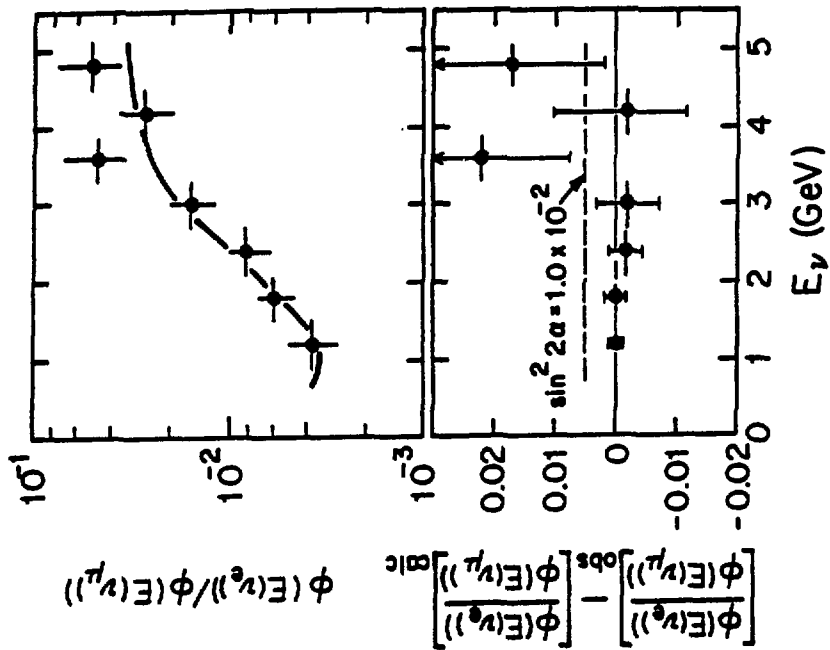


Fig. 8a. Ratio of ν_e/ν_μ flux as a function of E_ν ;
 b. The difference of the calculated and measured ν_e/ν_μ flux ratios as a function of E_ν .

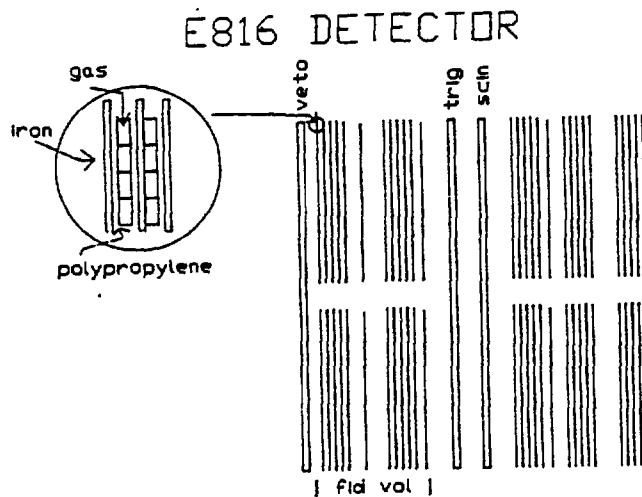


Fig. 9a. The E816 detector.

events (23 ± 8), corresponding to a ν_e/ν_μ rate of $(2.0 \pm 0.5)\%$ was observed. Since the CERN PS beam was no longer available, the group moved their detector to BNL to continue their investigation of the observed ν_e excess. At Brookhaven the L/E_ν was very similar to the value at CERN. However, the flux in the new run was more than five times that in the original experiment and a significant amount of antineutrino data was also taken. The detector used at BNL (Fig. 9) was an improved version of the CERN detector. In addition, a number of possible biases such as the trigger used and the location of the detector off the beam axes were eliminated.

The detector primarily consists of flash-tube chambers separated by 3mm thick iron plates. Each flash tube is 6m x 5mm x 5mm and they are assembled into 6m x 3m arrays between a pair of iron plates. A plane of the detector consists of two of these arrays. In the target region of the detector the planes are combined into 5 plane modules and four such modules are stacked to produce a 6m x 6m array, 10 planes deep. Each plane is $\approx 17\%$ of a radiation length and the total target mass is 10mton. The rest of the detector consists of 6 similar modules stacked again into 6m x 6m arrays. In this case the modules have 1 radiation length lead sheets between the planes to provide good shower containment. The total depth of the detector is 15 radiation lengths. All of these tubes are y-measuring tubes and at CERN there was no x-measuring information. For the run at BNL a few additional individual planes were built and these provided limited x-information. In front of the target detector was a plane of liquid scintillator calorimeters which served as a veto array. After the target detector were 2 trigger planes of scintillation counters. The experiment trigger consisted of no signal in the veto plane and a coincidence between the trigger planes in which the threshold was low enough to yield high trigger efficiency for a single minimum ionizing track.

Approximately 500,000 (100,000) triggers were recorded during a neutrino (antineutrino) run of 1.1×10^{19} (1.3×10^{19}) protons on

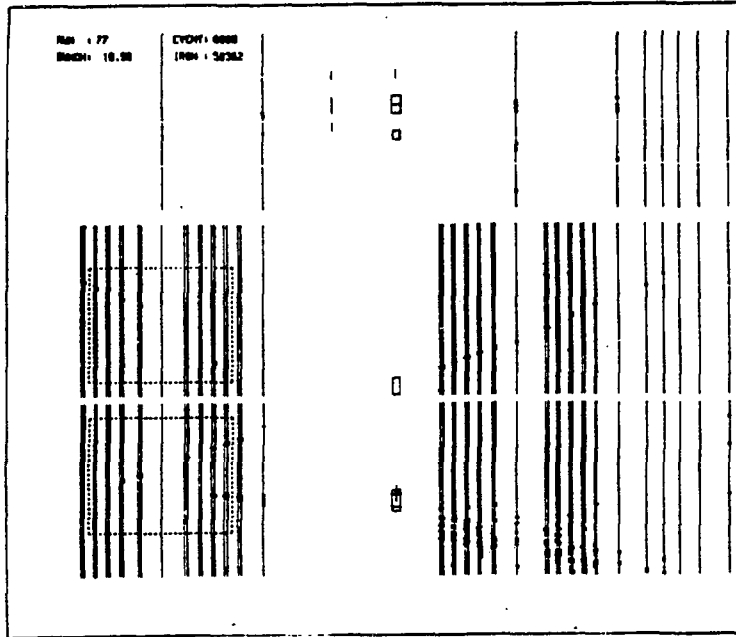


Fig. 10. Example of a real event with a hadron or muon track and a disconnected shower.

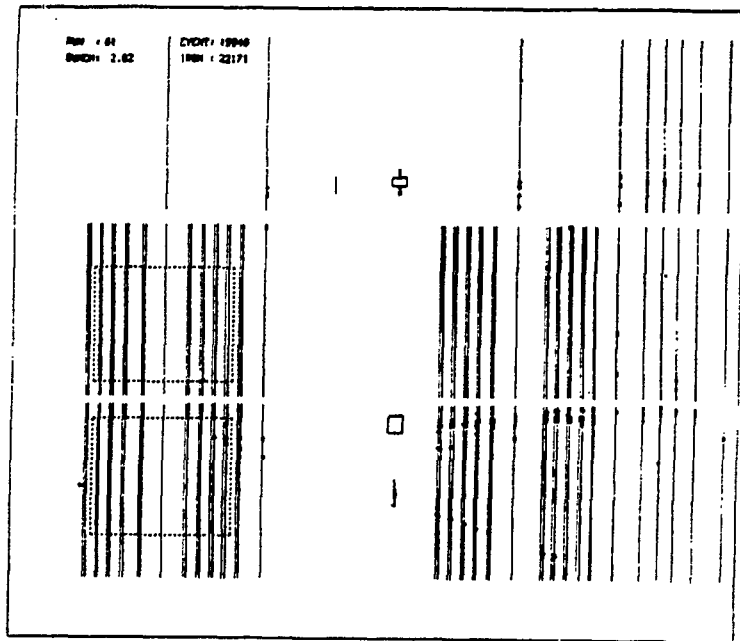


Fig. 11. Example of a real event with hadron or muon track and a connected shower.

target. A simple software filter rejects half of the triggers and the present preliminary results are based on a scan of about 1/3 of the neutrino data (0.4×10^{19} protons on target).

The purpose of the scan was to select 2 or 3 track events with or without associated electromagnetic showers. It is not possible, because of the lack of a good second projection to work with the simplest (single track) topology. In addition the small size of the detector does not afford good muon identification, while the lack of dE/dx information prevents π/p separation. Consequently, the analysis is based entirely on topological and shower information. The shower energy calibration gives approximately 120 tubes fired per GeV of energy.

The normalization for the experiment is determined by comparing the observed 2 and 3 track events found in the scan with those predicted by a Monte Carlo calculation. In this calculation the calculated beam spectra and the known quasi-elastic and pion production cross sections were used to generate events. These events were simulated in the detector and processed. A total of 3334 2-track events were found in the data scan while the analysis of the Monte Carlo data predicted 3226 such events. There is good agreement in the length and opening angle distributions between the real and Monte Carlo events.

Electromagnetic showers were identified by their characteristic shower-like hit pattern. Fig. 10 is an example of an event with a shower disconnected from the primary event vertex while Fig. 11 shows a connected shower event. The validity of the scanning criteria for selecting showers and the likelihood of π, p or μ faking an electron shower was determined from test beam measurements of e, π, p, μ using the real detector in an AGS test beam. With the requirement that the shower have > 50 hits there is a very small probability that the showers are not genuine. The events with showers were separated into those with only one visible shower and those with two separate showers. This latter class was defined to be π^0 events and was used to study the properties of showers in the detector. The number of

observed π^0 events was 54 ± 7 while the same Monte Carlo used for the normalization calculation predicted 55 ± 8 events. The disconnection distance (the distance in the beam-direction from the event vertex to the conversion point of the shower) for the Monte Carlo events is shown in Fig. 12b and for the data in Fig. 13b. The agreement is good with a slope consistent with the radiation length for the detector. Events with one visible shower may actually be two shower events where the showers overlap in the visible projection and are not distinguishable. To simulate this effect, only the connection distance for the closest shower in the π^0 events is plotted in Fig. 12c and Fig. 13c. As expected, the slope is much steeper and within the limited statistics the agreement between Monte Carlo and data is acceptable. In Fig. 12a, Fig. 13a are plotted the disconnection distances for Monte Carlo and data events, respectively, in which there is a track and only one shower. The Monte Carlo distribution shows no excess at small conversion distance and the slope of the distribution is between the values for the distributions with 2-showers (Fig. 12b) and with only the first conversion (Fig. 12c) as expected. The real data (Fig. 13a), on the other hand, has a significant excess in the first bin. If the first bin is excluded from the fit, the slope in this case is very consistent with that from the Monte Carlo data. The fit to the conversion distance distribution, excluding the first bin, predicts 31 connected showers from π^0 events while there are a total of 93 events in the first bin. From the calculated ν_e/ν_μ ratio in the beam (8×10^{-3}) and the observed charged current events the expected number of ν_e beam events with one track and one shower is 27. The excess of electron events is therefore 35 with a statistical error of ≈ 12 . At this stage of the analysis there is no estimate of the systematic error. However the collaboration believes that the present significance is $\approx 3\sigma$. Furthermore, the present ratio of excess electrons to charged current events is similar to that measured in the earlier CERN PSI91 experiment and is consistent with the $\Delta m^2 - \sin^2 2\alpha$ region shown in Fig. 2. Work is continuing both on the analysis of

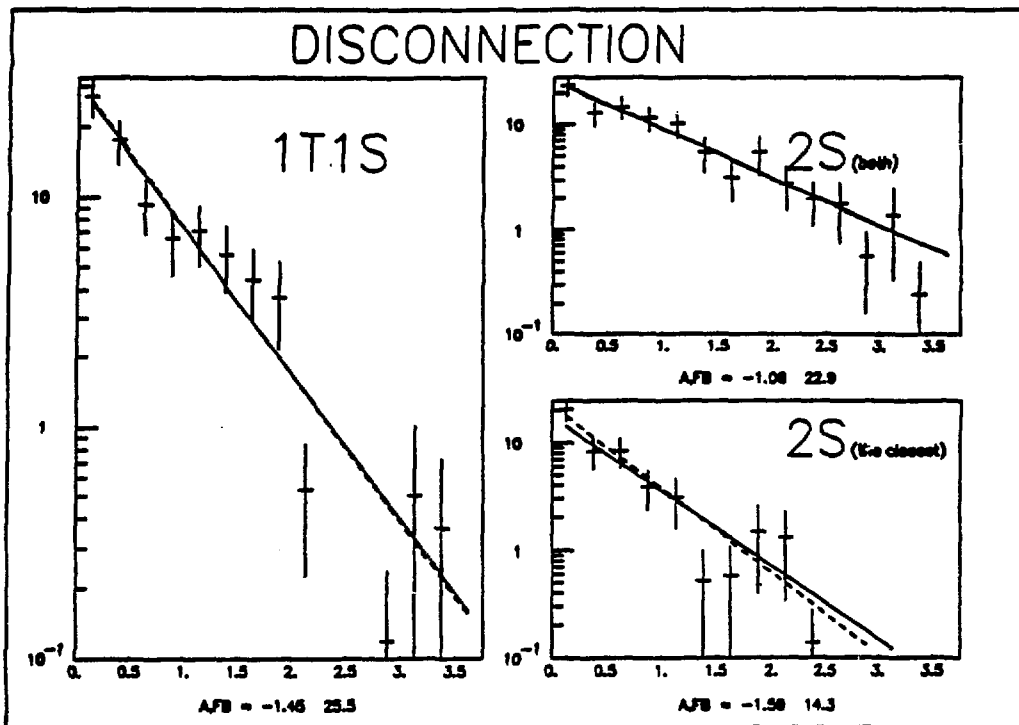


Fig. 12. Distributions of disconnection distances in radiation lengths for Monte Carlo events (a) Events with one track and one shower; (b) Events with 2 showers. Distance for both showers plotted; (c) Events with 2 showers. Only distance for closest conversion plotted.

the remaining 2/3 of the neutrino data and all of the antineutrino data and on understanding the systematic errors in the experiment.

7. THE E776 $\nu_\mu \rightarrow \nu_e$ OSCILLATION EXPERIMENT

Experiment 776, a Columbia Univ., Univ. of Illinois, Johns Hopkins Univ. collaboration, is an experiment at BNL to search for $\nu_\mu \rightarrow \nu_e$ oscillations with a detector located at $\approx 1000\text{m}$ from the neutrino production target using a narrow band beam with $\langle E_\nu \rangle = 1.27$ GeV. This experiment has $L/E_\nu \approx 1$ which is similar to the BEBC experiment discussed above. In principle a narrow band beam has advantages for a $\nu_\mu \rightarrow \nu_e$ oscillation search. The beam is made by

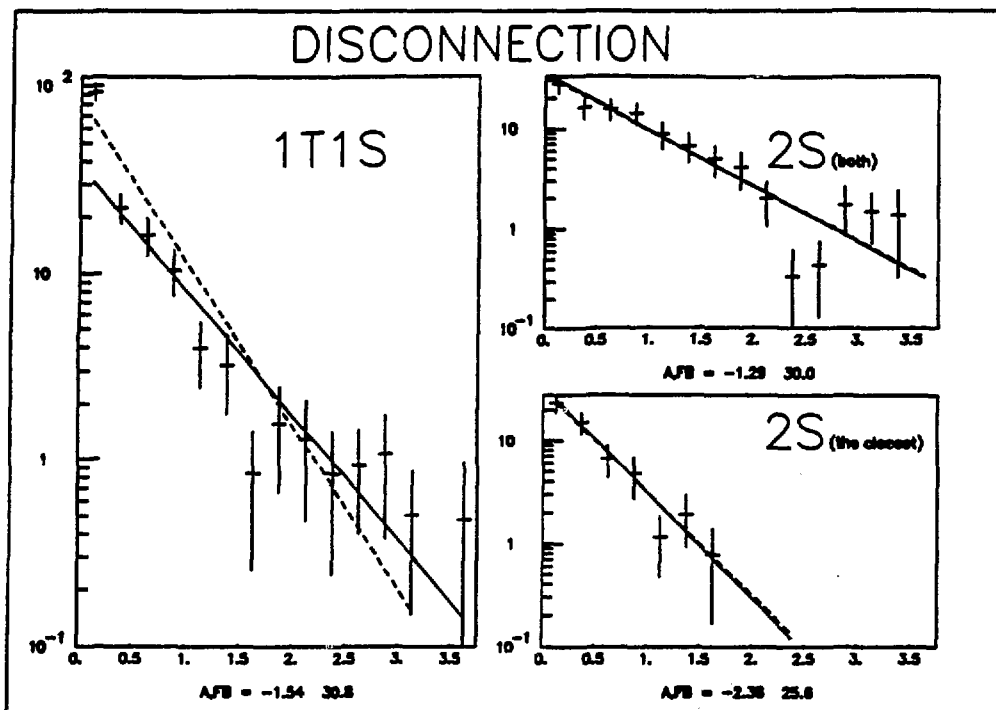


Fig. 13. Distributions of disconnection distances in radiation lengths for real events (a) Events with 1 track and 1 shower; (b) Events with 2 showers. Distances for both showers plotted; (c) Events with 2 showers. Only distance for closest conversion plotted.

momentum selecting the produced pions and kaons ($P_{\pi,K} \approx 3 \text{ GeV}/c$ for this beam). The resulting decays produce a dichromatic neutrino beam with a dominant pion peak ($E_{\nu\pi} \approx 1.27 \text{ GeV}$), a small kaon peak and a reduced wide band continuum arising predominantly from π/K decays before the momentum selection is complete. This is significantly different from the ν_e beam contribution from 3-body $K \rightarrow \pi\nu_e$ decays which has a much broader spectrum and no dichromatic structure. Any oscillation signal should mirror the ν_μ dichromatic structure and be clearly distinguishable from the 3-body K -decay spectrum. In practice the advantages of the narrow band beam compared to a wide band beam are not so apparent. Since the narrow band flux is at best a few percent of the wide band flux, it is difficult to attain good statistics at large distances. Furthermore, at BNL energies, the

240 kA ν_μ and ν_e Beam Energy Distributions

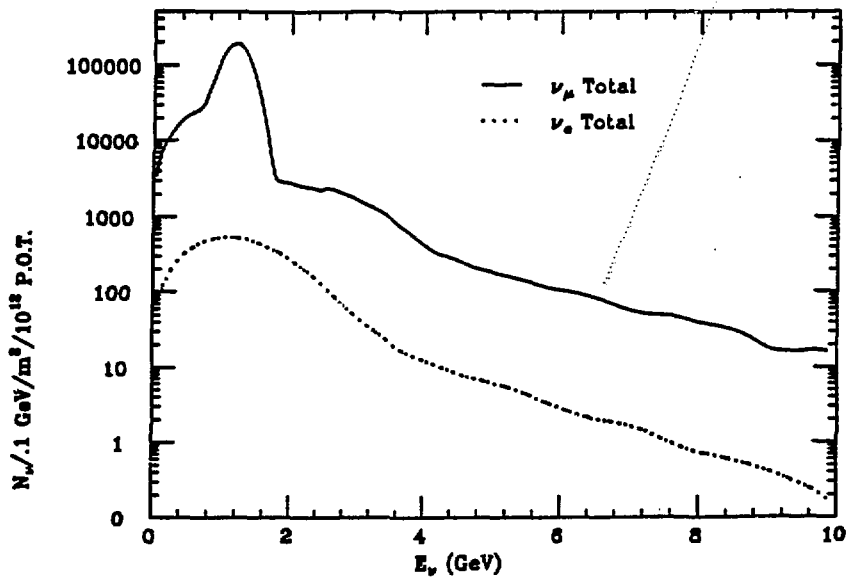


Fig. 14. Calculated ν_μ and ν_e spectra for the E776 narrow band beam at the detector location ($\approx 1000\text{m}$).

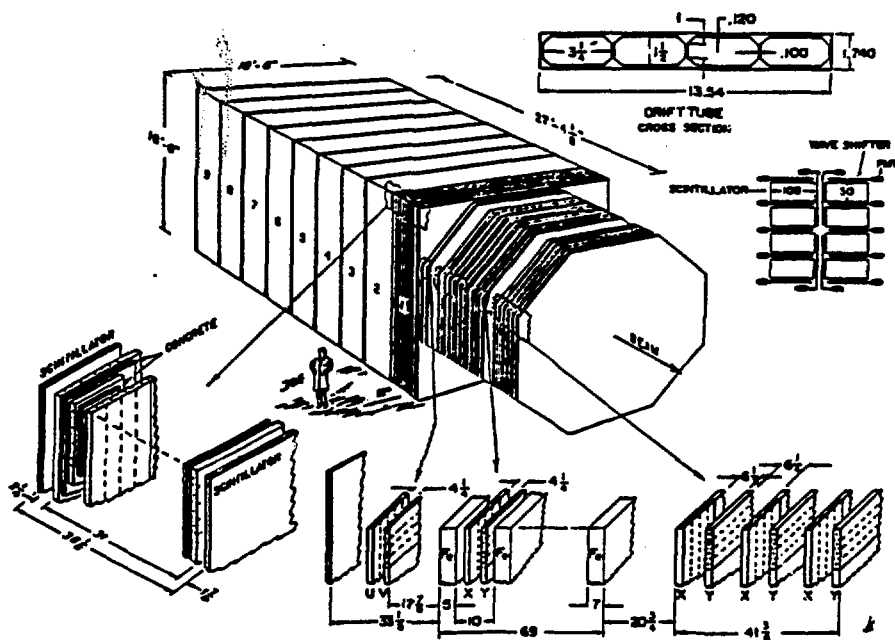


Fig. 15. The E776 detector.

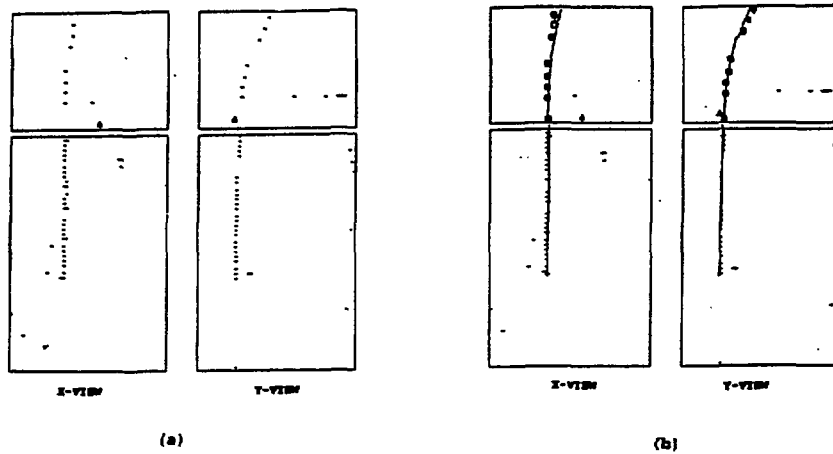


Fig. 16a. A μ^- candidate which passes through the toroids;
 b. The reconstructed track for this μ^- candidate.

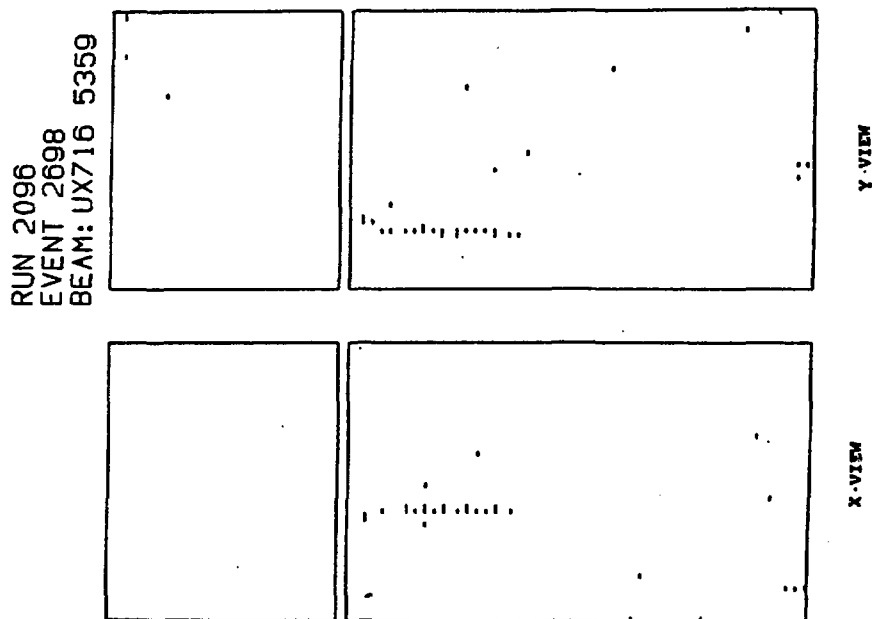


Fig. 17. An electromagnetic shower candidate.

dominant source of ν_e flux is $\pi \rightarrow \mu \rightarrow \nu_e$ decays and not 3-body K-decays. These π -decays cause the expected ν_e flux to peak under the narrow band ν_μ peak.

The calculated ν_μ and ν_e spectra for the narrow band beam used in this experiment are shown in Fig. 14. The beam is monitored by two sets of ionization counters located in the decay tunnel 48m and 60m from the production target. The radial distribution in these detectors is in agreement with the Monte Carlo expectations and the absolute number of minimum ionizing particles passing through the monitors agrees to $\leq 30\%$. While the monitors do not provide a measure of the relative π/K content in the beam or energy information on the produced particles, they are a good monitor of the normalization, and the overall stability of the beam.

The E776 detector is a 250 ton (120 ton fiducial volume) target calorimeter made of 9 supermodules (18 ft. x 18 ft. in cross section) followed by a spectrometer of magnetized iron toroids (Fig. 15). Each supermodule contains 5 modules followed by a plane of scintillator for precise event timing. Each module contains a plane of 1" thick concrete, a plane of x-measuring proportional drift tubes (PDT), another plane of 1" thick concrete and a plane of y-measuring PDT's. The sampling thickness is $\approx 1/3$ of a radiation length. There are 64 PDT tubes per plane and the charge information from each wire is digitized using flash ADC's. These ADC's are 8 bits with 22.4 nsec sampling so they record the charge history for $\approx 6 \mu\text{sec}$. A typical quasi-elastic μ^- candidate in the detector is shown in Fig. 16 while an electron candidate is shown in Fig. 17. The electron has a distinctive hit pattern compared to the typical muon or pion track. The ADC information from the hit wires in the first few planes for the muon and electron track is shown in Fig. 18. While the muon track, apart from occasional δ -rays, has a regular and small ionization loss, increased ionization and gappiness is apparent on the electron track.

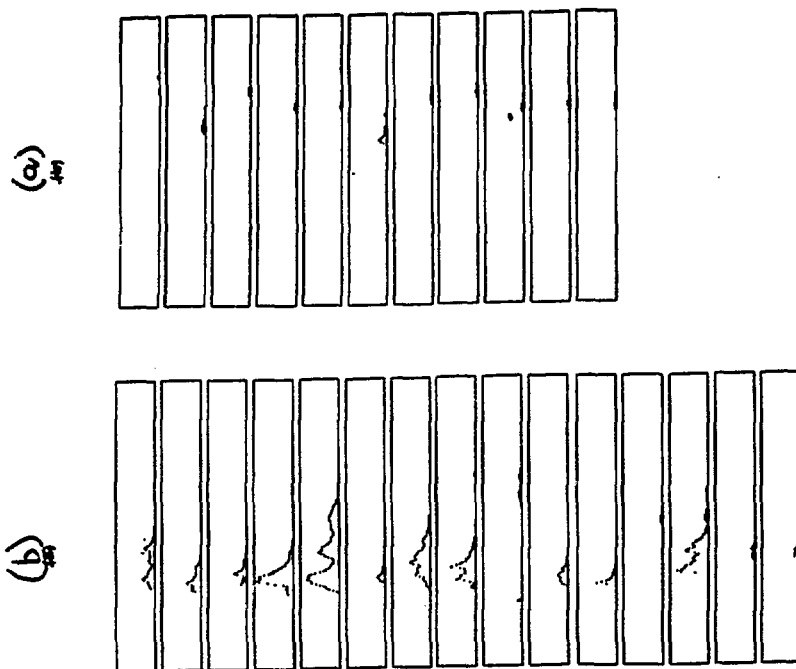


Fig. 18. Flash ADC information for the first few wires hit from, (a) The μ^- candidate in Fig. 16; and (b) The e^- candidate in Fig. 17.

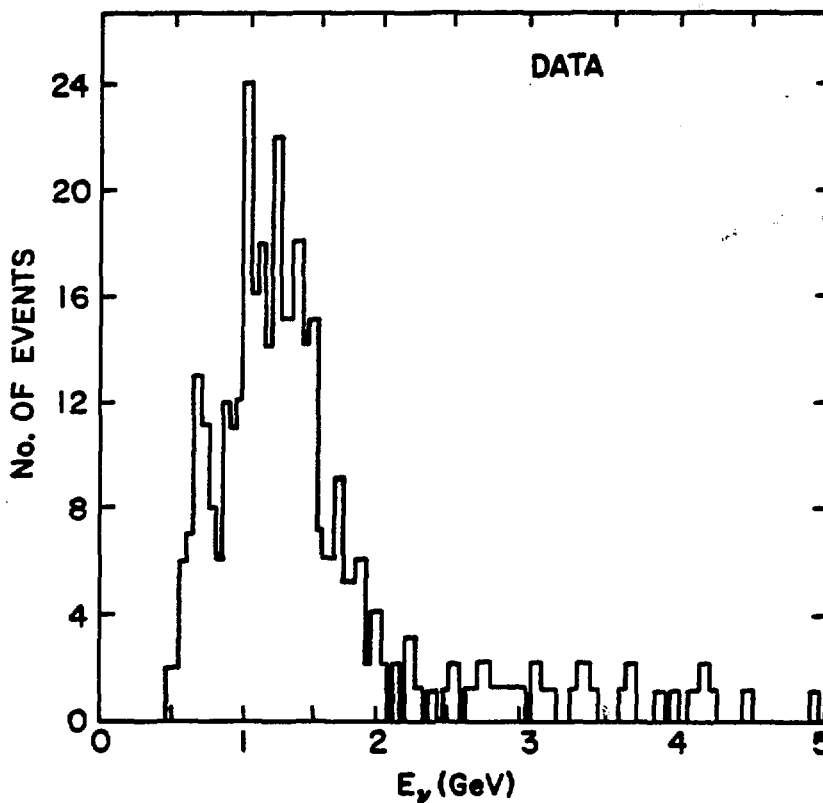


Fig. 19. The E_ν distribution calculated using the observed μ^- tracks from quasi-elastic events ($\nu_\mu n \rightarrow \mu^- p$).

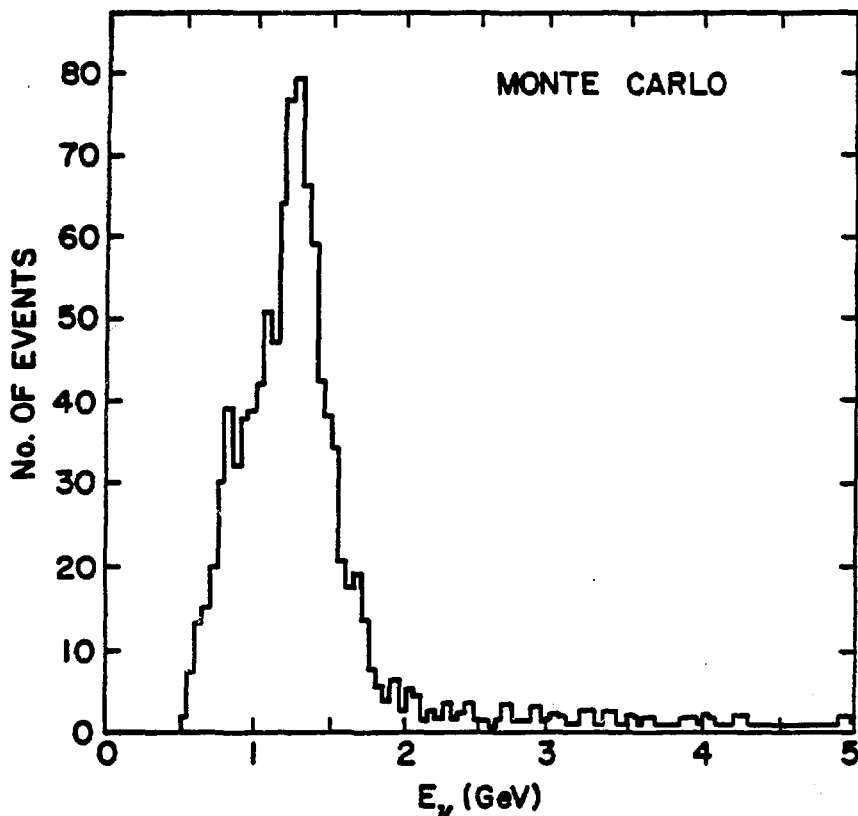


Fig. 20. The expected $E_{\nu\mu}$ distribution for quasi-elastic events from a Monte Carlo calculation.

The identification of electromagnetic showers and the rejection of μ, π, p tracks as shower candidates in this detector were studied with an identical test detector using e, π, μ, p tracks of various momenta from an AGS test beam. The algorithms developed were based on gaps in the hit pattern, the average number of ionizing tracks per PDT and the longitudinal and transverse fluctuations of the track. At this stage of the analysis the μ, p, π contamination in the electron sample is believed to be very small.

The data taken in this experiment consists of 1.85×10^6 beam pulses and corresponds to 3×10^{19} protons on target. Since the event rate is low, an equivalent number of "free" pulses (i.e. pulses equivalent in length to the beam pulses but out of time) were taken to study possible cosmic ray backgrounds to the real events.

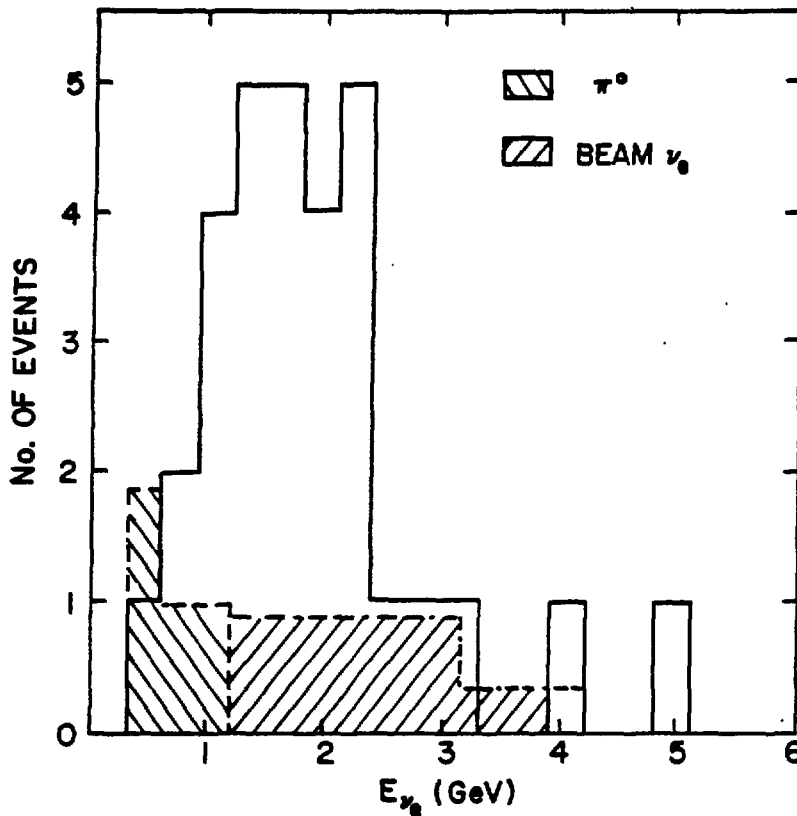


Fig. 21. The calculated neutrino energy distribution for the observed e^- tracks from quasi-elastic events ($\nu_e n + \mu^- p$) and the estimated background from beam ν_e events and ν_μ induced π^0 events.

An initial software filter was used to select 323×10^3 bursts which had potential neutrino candidates in the fiducial volume. A series of scans were then carried out to select one or two track events which were good candidates for quasi-elastic $\mu^- p$ or $e^- p$ final states. This reduced the data to a sample of 1406 "μ" type events and another of 917 "e" type events. The sample of $\mu^- p$ candidates was further refined by requiring that the muon track be within 50° of the nominal neutrino direction and that the muon momentum be measurable either from range or by curvature in the spectrometer. The final sample consisted of 614 single track $\mu^- p$ candidates or 860 < 2 track $\mu^- p$ candidates. From a study of the "free" triggers it was determined that $\lesssim 1.5\%$ of these events could be due to cosmic ray background. The calculated E_ν spectrum for these events, assuming they are real quasi-elastic, is shown in Fig. 19 while the expected distribution

calculated from the beam spectra and the known quasi-elastic cross section is shown in Fig. 20. The overall agreement is quite good but there is a significant excess at high energy in the real data compared to the Monte Carlo. The average quasi-elastic acceptance for the selected events is $\sim 10-15\%$.

The initial shower candidates were further refined using the shower criteria and hadron track rejection cuts discussed above. For this analysis the real data was supplemented by Monte Carlo ν_e and ν_μ induced π^0 background events. The combined sample was processed through the various edit, scan, measuring and analysis stages. In this way the acceptances and backgrounds were determined. The π^0 background in the final ν_e sample was determined from the number of $\pi^0 \rightarrow \gamma\gamma$ where both γ 's were observed in the detector (1 (4) events for 1 (≤ 2) track events) and the Monte Carlo acceptance for observing both gamma from the π^0 compared to observing a single γ faking an electron shower. Since this relative acceptance is ~ 1 (actually 7/9), the expected background from π^0 events is 1 (4) events for one track (≤ 2 track) candidates.

The number of events expected from ν_e in the beam is determined from the number of ν_μ events observed, the relative e to μ acceptance (≈ 1) and the calculated ν_e/ν_μ ratio for this beam (8×10^{-3}). For one track (≤ 2 track) events the background is 5 (7) ν_e induced events. Since the actual number of electron events found was 22 (36) one track (≤ 2 track) events and the combined π^0 and ν_e backgrounds amount to only 6 (11) events there is a clear excess of 16 (25) electron events with one (≤ 2) tracks in the final state. The neutrino energy distribution calculated for the electron candidates and the estimated backgrounds are shown in Fig. 21. At present the systematic errors on the background estimates are not known but the collaboration believes that the effect will be $\geq 3\sigma$ and the excess rate of electron events compared to muon events is $\sim 2 \times 10^{-2}$. The approximate range in Δm^2 , $\sin^2 2\alpha$ allowed by this conclusion is indicated in Fig. 2. It should be noted that the energy distribution of the final electron events (Fig. 21) is peaked higher than the ν_μ beam spectrum (Fig. 19) whereas one would expect an oscillation signal

to peak under the ν_μ beam peak. It is believed that at least part of this discrepancy is due to the difference in energy resolution for muon and electron events. Work is continuing on the analysis of this experiment and final results will be available in the not too distant future.

8. LONG BASELINE $\nu_\mu \rightarrow \nu_e$ OSCILLATION SEARCHES

Present $\nu_\mu \rightarrow \nu_e$ oscillation searches at accelerators are limited by their L/E_ν range (0.1-1) to $\Delta m^2 \gtrsim 0.1 \text{ eV}^2$ and $\sin^2 2\alpha \gtrsim 5 \times 10^{-3}$. It appears possible with the advent of the Booster to significantly improve the Δm^2 range to perhaps $\Delta m^2 \gtrsim 0.01 \text{ eV}^2$ while maintaining reasonable $\sin^2 2\alpha$ coverage. However for a reasonable amount of Booster running ($\approx 10^{20}$ POT) with a modest detector (1 Kton fiducial volume), it is difficult with distances greater than 10 Km to retain acceptable $\sin^2 2\alpha$ coverage.

The rate of detected μ^- tracks with $\theta_\mu < 30^\circ$ and $P_\mu > 350$ MeV/c from $\nu_{\mu n} \rightarrow \mu^- p$ quasi-elastic events in the E734 detector is $4 \times 10^{-2} \mu^- / 10^{13}$ POT/30 mton. This corresponds to only $\approx 15\%$ of the total event rate but for a good $\nu_\mu \rightarrow \nu_e$ search is a reasonable estimate of the usable events in the detector. For distances > 1 Km this rate is given by $N = 20 \times M / L^2$ where M is the detector fiducial mass in mton, L is the source to detector distance in Km and N is the observed number of quasi-elastic muons for 10^{19} POT. This rate assumes a $1/L^2$ beam dependence which is reasonable for $L > 0.5$ Km and is obtained by explicitly correction for the measured E734 rate at 100m.

Recent AGS neutrino running has averaged 10^{19} POT per 3 calendar weeks. If the Booster increases the rate by a factor of 4, then a run of 10^{20} POT appears quite reasonable. The observed μ^- quasi-elastic rates for a 1 Kton fiducial volume detector with a 10^{20} POT run are given in Table 1. the expected e^- quasi-elastic rates for an e/μ ratio of 1% are also listed.

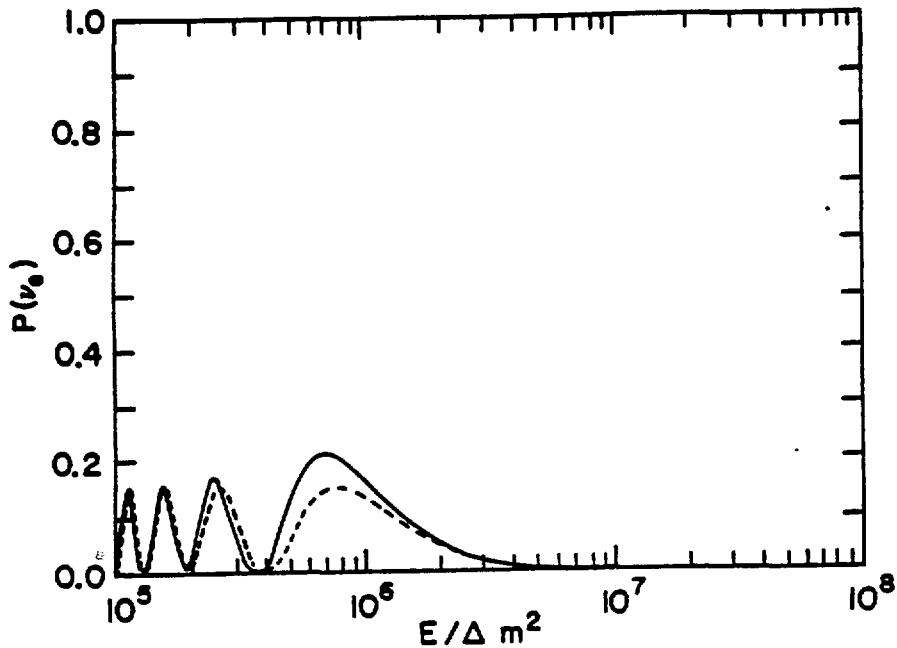


Fig. 22. Probability for ν_e events due to oscillations as a function of $E(\text{MeV})/\Delta m^2(\text{eV})^2$ at 1000 Km taken from a calculation by A. Baltz, J. Weneser (Ref. 1). Dashed curve is for vacuum oscillations only while the solid curve includes matter enhancement from passage through the earth.

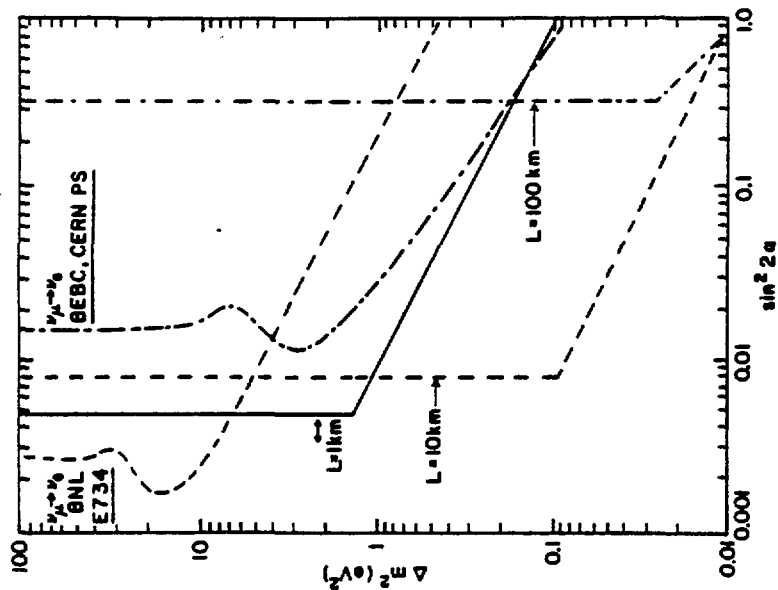


Fig. 23. Estimated $\nu_\mu \rightarrow \nu_e$ oscillation limits for various source to detector distances (L) for a 1 Kton fid. vol. detector and 10^{20} protons on target.

TABLE 1

Observed Rates for 10^{20} POT with 1 Kton Fiducial Volume Detector

<u>L(Km)</u>	<u>#μ^-(μ^-p)</u>	<u>#e^-(e^-p)</u>
1	2×10^5	2×10^3
10	2×10^3	20
100	20	.2
1000	.2	.002

The rate beyond 10 Km is discouraging. This is unfortunate because one might hope that with sufficient distance matter oscillation effects might become significant. However, even at 1000 Km (Fig. 22) the matter effect is insignificant and at this distance the rate is negligible.

If one assumes that the large detector used in this search has approximately the electron identification and photon rejection capabilities of the E734 detector, then it is straightforward to calculate the expected oscillation limits (Fig. 23). As is clear from these limits, the lack of statistics beyond 10 Km severely restricts the $\sin^2 2\alpha$ limit and the increased distance does not substantially aid the Δm^2 limit. Consequently, even with the added flux of the booster it is unlikely that searches much beyond 10 Km will be effective. On the other hand, there is every possibility of significantly extending the present $\nu_\mu \rightarrow \nu_e$ oscillation searches. Clearly any experiment which improves $\nu_\mu \rightarrow \nu_e$ searches should be able to improve on ν_μ disappearance searches but it is more difficult to estimate the expected limits in this case.

CONCLUSIONS

The Brookhaven Neutrino Workshop was an active forum for the presentation of theoretical and experimental results in $E_\nu \approx 1$ GeV neutrino physics and for the discussion of future options in this area. No significant new initiatives for non-oscillation experiments

were proposed. The major interest in the workshop was on $\nu_\mu \rightarrow \nu_e$ oscillation searches at accelerators.

The present situation with regard to $\nu_\mu \rightarrow \nu_e$ oscillations at accelerators is confused. While one must wait for final results from E816 and E776 before drawing conclusions, it appears unlikely that all of the present positive signals will disappear. If a reasonable positive signal remains, it will be necessary to establish the oscillation nature of the signal. This will require an experiment with two similar detectors at two different distances to establish the L/E_ν behavior of the electron excess. With the increased flux provided by the booster, it should be feasible to build modest tonnage detectors with active fiducial volumes and high segmentation for this second generation experiment. If no signal is confirmed it should be possible to significantly decrease the present limits with a new, much larger, detector at $\approx 10\text{Km}$.

This work has been supported by the U.S. Department of Energy under contract DE-AC02-76CH00016.

REFERENCES

1. Proceedings of the Brookhaven National Laboratory Neutrino Workshop, BNL, Upton, NY, Feb. 4-6, 1987, Ed: M.J. Murtagh, in press.
2. Booster Design Manual, Accelerator Development Dept. Brookhaven National Laboratory, 10/29/86.
3. "Elastic Scattering of Muon Neutrinos at BNL". E734 collaboration, (Presented by S.L. Durkin) APS Division of Particles and Fields Meeting, Salt Lake City, UT, Jan. 1987, to be published;
L.A. Ahrens, et al. Phys. Rev. Lett. 58, 636 (1987).
4. Derrick, M. et al. "Evidence for the Decay $\tau^+ \rightarrow \pi^+ \eta \bar{\nu}_\tau$ ". ANL-HEP-PR-86-106, Feb. 1987 (Submitted to Physics Letters).
5. E816 (A Boston Univ., BNL, CERN, Paris collaboration) Presented by P. Astier, LPNHE, Paris, see Ref. 1.

6. E776 (A Columbia Univ., Univ. of Illinois, Johns Hopkins Univ. collaboration) Presented by G. Tzanakos, Columbia Univ., see Ref. 1.
7. Ahrens, L.A. et al. Phys. Rev. D31, 2732 (1985).
8. Angelini, C. et al. Phys. Letts. B179, 307 (1986).
9. Bernardi, G. et al. Phys. Letts. B181, 173 (1986).